46th AIAA Aerospace Sciences Meeting and Exhibit
7 - 10 January 2008, Reno, Nevada

AIAA 2008-1396

Electromagnetic Boundary Layer Flow Control Facility Development Using Conductive Particle Seeding

Eric M. Braun,[*] Richard R. Mitchell, [*] Akihiro Nozawa,[†] Donald R. Wilson,[‡] and Frank K. Lu[§]
University of Texas at Arlington, Arlington, Texas, 76019

and

J. Craig Dutton[**]
University of Illinois at Urbana-Champaign, Champaign, Illinois, 61820

A facility for electromagnetic boundary layer flow control employing conductive particle seeding is in the initial stages of development, fabrication and testing. The facility consists of three integrated components: a conductive particle seeding mechanism, an ionization plate and a Lorentz force generator plate that comprises of a series of flush-mounted surface electrodes and embedded rare earth magnets. Initial bench-top testing is reported with the future intention of testing the facility in the low speed and supersonic flow regimes. An aqueous salt solution reduced the voltage required to create a corona discharge by the ionization plate. The ionization of seeded air by an electric field presents several problems, notably an increased tendency for arcing as the conductivity within the boundary layer increases. The aqueous salt solution was accelerated or decelerated by the Lorentz force generator depending on the electromagnetic configuration. The benchtests demonstrated the ability of raising the conductivity of air to enable Lorentz force actuation under normal atmospheric conditions.

Nomenclature

a	=	acceleration, m/s^2
B	=	magnetic field strength, T
E	=	electric field potential, V/m or N/C
F	=	force, N
I	=	current, A
I_M	=	interaction parameter
I_M^*	=	modified interaction parameter
J	=	current density, A/m^2
l	=	characteristic length, m
L	=	Lorentz body force, N/m^3
m	=	mass, kg
N	=	positive magnetic pole
R	=	resistance, Ω
S	=	negative magnetic pole
U	=	flow speed, m/s
U_∞	=	free stream flow speed, m/s

[*]Graduate Research Associate, Aerodynamics Research Center, Department of Mechanical and Aerospace Engineering, Box 19018. Student Member AIAA.
[†]Undergraduate Research Assistant, Aerodynamics Research Center, Department of Mechanical and Aerospace Engineering, Box 19018. Student Member AIAA.
[‡]Professor and Chair, Department of Mechanical and Aerospace Engineering, Box 19018. Associate Fellow AIAA.
[§]Professor and Director, Aerodynamics Research Center, Department of Mechanical and Aerospace Engineering, Box 19018. Associate Fellow AIAA.
[**]Professor and Chair, Department of Aerospace Engineering. Associate Fellow AIAA.

U^* = friction velocity, m/s
V = voltage, V
x = Cartesian coordinate along streamwise direction
y = Cartesian coordinate along spanwise width
z = Cartesian coordinate along transverse height
δ_{BL} = boundary layer thickness, mm
μ = gas viscosity
ρ = gas density, kg/m^3
σ = gas conductivity, mho/m
τ = shear stress, N/m^2
φ = electric scalar potential
ψ = magnetic scalar potential
∇ = gradient

I. Introduction

RECENT interest in gas dynamics applications of electromagnetic forces has been for magnetohydrodynamic (MHD) accelerators and power generators for hypersonic vehicles, turbulence suppression, boundary-layer control and high-speed vehicular control.[1-5] In particular, electromagnetic control concepts have been proposed to replace present high-speed aerodynamic vehicle control methods that involve the actuation of large, bulky control surfaces or the use of reaction jets. These existing methods have adverse consequences in high-speed flight, such as high surface loading, high heating and flow unsteadiness, or they may cause undesirable aerodynamic interference with other vehicular components. An innovative approach to avoid the difficulties of conventional aerodynamic actuation is presented in this paper. This new technique is lightweight, compact and requires low power.

There are two general approaches for utilizing electromagnetic (Lorentz) forces for flow control: electric field only, also known as plasma flow control, and a combination of electric and magnetic fields. Solely applying an electric field causes plasma to either accelerate or decelerate depending on the electrode arrangement, thereby distorting the flow field to produce a virtual aerodynamic surface.[6] However, the distortion appears to be too small for use in the high dynamic pressure environment of high-speed flows. Another approach is to modify the flow through volumetric energy addition. Present attempts at trying to affect the flow volume, however, are plagued with difficulties in energy deposition.[7]

The electromagnetic flow control (EMFC) approach utilizes electromagnetic (EM) interactions to manipulate an air flow ionized by seeding it with electromagnetically conducting particles. Theoretical studies have shown that EMFC can provide control forces and moments comparable to those produced by a traditional flap through distorting the flow but without the penalties of large power consumption, bulk and weight. Adverse effects such as increased drag or localized heating are also reduced with EMFC. The EMFC concept is also fast-acting, a feature that is desirable for high-speed flight. However, EMFC concepts examined thus far exhibit poor fluid/EM coupling.

The second approach involving MHD interactions between a weakly ionized gas and electromagnetic fields also entails volumetric or surface interactions as in plasma flow control. Volumetric interactions have primarily centered on demonstrating the AJAX concept for hypersonic propulsion[8] or MARIAH, a hypersonic test facility concept that incorporates an MHD flow accelerator.[9] MHD interactions appear to be promising for high-speed aerodynamic applications since they scale quadratically with the magnetic field strength according to the interaction parameter $I_M = \sigma B^2 l / \left(\rho U_\infty\right)$.[1] However, existing magnet technology makes volumetric MHD concepts impractical for aerodynamic applications since high-strength magnets producing 1-5 T (such as those used in magnetic resonance imaging) are massive and bulky. More modest surface MHD interactions have also been proposed[10] and have been demonstrated at low speeds in salt water.[11] This approach, however, has not been well studied for high-speed aerodynamic flow with only some work reported recently.[10,12-14]

Two parameters govern the electromagnetic interaction of the weakly-ionized gas flows of interest here, namely, the interaction parameter $I_M = \sigma EBl / \left(\rho U_\infty\right)$ and the Hartmann number $Ha = Bl\sqrt{\sigma/\mu}$. For high-speed flows, the value of I_M is ostensibly small due to the low value of σ and the large flow speed. Hence, volumetric EMFC may be problematic. However, localized boundary-layer control, as proposed here, appears more promising since only local ionization is needed near the surface where the velocity and density are low, and where electromagnetic fields are most intense. The non-linear coupling between the boundary layer flow and the electromagnetic fields can significantly influence the local flowfield.[11,15] Instead of I_M, an interaction parameter based on boundary-layer

scales appears more appropriate, namely, $I_M^* = \sigma EBl \Big/ \left(\rho U^{*2}\right)$, where $U^* = \sqrt{\tau_w / \rho_w}$ is the friction velocity and where the subscript w refers to wall values.[7] The parameter I_M^* can be nearly 300 times that of I_M, thereby raising the possibility of practical EMFC.

Based on the observations above, the combined electromagnetic approach for aerodynamic, boundary layer control appears promising for aerodynamics because it can yield large values of I^*. Two immediately obvious strategies involve raising the electric and magnetic field strengths. However, the electric field strength cannot be too excessive as arcing would otherwise occur. A reasonable value of E for producing the onset of a glow discharge of charged particles (also known as corona discharge) appears to be 50 kV/m.[16] As for achieving a strong magnetic field, high-strength superconducting magnets are impractical for aerospace applications because of their bulk and mass. An upper bound of $B < 1$ T can be achieved by permanent, rare earth neodymium magnets of acceptable mass and size. Finally, other than raising the electric and magnetic field strengths, there remains the possibility of raising the plasma conductivity through artificially seeding the flow, which may hold the key to successful implementation of EMFC of high-speed, aerodynamic boundary layers. For example, cesium carbonate powder has been previously used to achieve conductivities of 1-10 mho/m in high-pressure aerodynamic plasmas.[17] This level of conductivity can be contrasted to the low value of 0.06 mho/m found in unseeded air plasmas at high-speed flight conditions.[14] Conversely, some of the theoretical and numerical work that demonstrates EMFC requires conductivities of up to 100 mho/m. This is unattainable in airflows unless they are artificially enhanced.

In order to obtain a so-called "cold plasma" with a high level of conductivity, electrically conducting particles can be introduced upstream of the EM field. Ionization of the particles must occur somewhere between the upstream injection and the EM field locations due to recombination effects. Additionally, particle size is a major issue. Particles as small as micron-sized cesium carbonate powder previously used still tend to settle out of the flow. Nanoparticles, unlike microparticles, have the tremendous advantage of large surface area density. The large surface area density is conducive to ionizing the particles through corona discharge instead of thermal ionization of the raw cesium carbonate which requires high temperatures. A proof-of-concept is proposed whereby the airflow is seeded by both dry, submicron particles with low ionization potential or by aqueous solutions of similar materials. This paper describes the general facility design and preliminary benchtests.

II. Low Speed Facility Design Considerations

The electromagnetic boundary layer flow control device can be divided into three major components: the conductive material injector, the ionization plate and the Lorentz force generator plate. These components are respectively labeled in Fig. 1 and shown as part of the low speed wind tunnel assembly. In the figure, the material injector is shown to be injecting dry alkali salt particles. For dimensional reference, each of the three component plates in Fig. 1 measure 6 in. × 8 in. The plates are interchangeable as part of another assembly designed for supersonic testing.

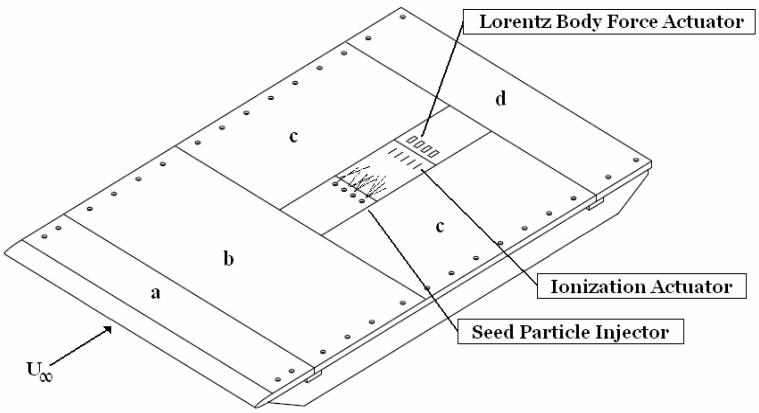

Figure 1. The EMFC test surface with major components highlighted.

The elliptical leading edge of the flat plate (plate *a*) has a fineness ratio of 0.3 as typically found for low-speed boundary layer investigations.[18-21] The EMFC device is located between the two filler plates labeled *c*. Additionally, a trailing edge plate *d* completes the assembly.

The experimental set-up is assembled in a closed circuit, low-speed wind tunnel with a closed test section. The test section is 61 cm high, 91 cm wide and 190 cm long (24 in. × 36 in. × 75 in.). The tunnel has a continuously variable speed capability from zero to approximately 50 m/s (160 ft/s). At the maximum operating condition, the tunnel is capable of obtaining a unit Reynolds number of 3 million/m (1 million/ft).

III. Conductive Particle Seeding

According to Jahn,[22] the extent to which magnetic body forces can be exerted on an ionized gas depends on the ability of the gas to conduct electric current. The body force due to the electromagnetic fields is given by

$$F_B = J \times B \tag{1}$$

where the current density is defined as:

$$J = \sigma\left(E + U_\infty \times B\right). \tag{2}$$

An examination of Eqs. (1) and (2) reveals that raising the conductivity of the gas will result in an increase in the body force. Therefore, several methods of raising conductivity are presented below.

The first method of increasing conductivity is by particle seeding. Particles may be delivered through two processes: (1) dry state via a nitrogen gas fluidized bed or (2) suspension in an insoluble liquid. These processes are shown in Figs. 2 and 3.

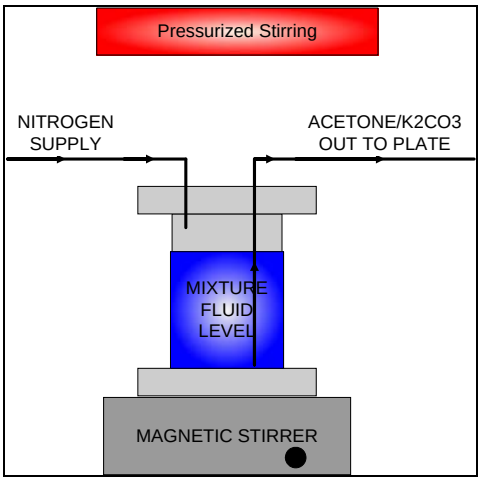

Figure 2. Pressurized injection system for liquid suspension.

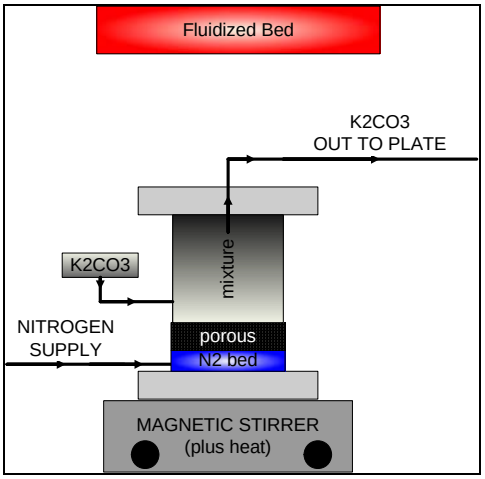

Figure 3. Heated and pressurized fluidized bed injection for dry seed.

The pressurized liquid injection seen in Fig. 2 delivers an aerosol mixture of potassium carbonate particles suspended in an insoluble liquid. Acetone and ethanol are two potential carriers. The fluidized bed injection, seen in Fig. 3, is an alternative process of delivery due to the flammability of the K_2CO_3 suspension. Both suspensions are being considered for future application. It can be noted that the choice of K_2CO_3 is primarily dictated by cost compared to the more active Cs_2CO_3.

For benchtesting of the Lorentz force plate and ionization plate, a solution of non-iodized sea salt and distilled water was used. The concentration of the solution was approximately 3 M (14.92 Wt.% NaCl). The ionic bonds of the sea salt compound completely dissociate when added to water, resulting in a solution that can easily conduct currents. The use of the salt/water solution was ideal for visualization of the Lorentz force plate actuation and ionization plate corona discharges.

IV. The Ionization Plate

An effective ionization plate must be capable of interacting with the ionized particles that it creates without arcing. Also, convection induced from the boundary layer flow or some other means must transport the ionized particles from the ionization plate to the Lorentz force plate a few cm downstream, as shown in Fig. 1. During the development process, several methods of ionization have been identified, each with benefits and drawbacks.

A method of ionization is to pass the seed particles though a high voltage DC electric field, known as field ionization. For this case, a strong electric field forcibly extracts an electron from an atom without the need for high current. By charge exchange ionization, electrons are exchanged with another atom through the outer valence shells.

The dimensions of the electrodes are dictated by the minimum separation distance required to prevent arcing.[23] Thin electrodes also tend to produce more of a corona discharge effect due to the concentration of charge on sharp surfaces. Using these principles, an ionization actuation plate was constructed with five electrodes (two positive, three ground) using approximately a one inch spacing between each. This is shown as a part of Fig. 9. A Glassman 20 kV power supply is used to generate the electric field. For the maximum voltage, the electrode spacing is close to the minimum requirement to prevent arcing (roughly one mm of separation per kV for air under ambient conditions). Since the seeded air has an elevated electrical conductivity, arcing is prone to occur (salt water solutions sprayed over the ionization generate a large amount of arcing). However, this situation can be alleviated by the velocity of the flow within the boundary layer. Simple experiments conducted thus far using the ionization plate show that an arc can be effectively "blown out" by a low-speed flow. Therefore, it is plausible that DC ionization of seeded air using a glow discharge can still take place without arcing although there may be a limited range of operation between conditions that suppress it while generating an appreciable amount of ionized particles.

Recent research involving ionization with high voltage fields[24,25] or magnetrons[26] has shown that pulsed electrical discharges may be superior to a DC discharge. Unlike DC, the pulsed discharges do not permit charge to build up on the surfaces of the electrodes which is a precursor to arcing. Depending on the success of the present DC field ionization attempts, the Glassman power supply can be linked to a high voltage semiconductor switch allowing for pulsed operation up to several hundred kHz. Square wave pulses at these frequencies should be more beneficial for this facility than RF pulses as will be discussed in the section on the Lorentz force generator and ionization actuator plate interaction.

Recombination of the ionized particles between the ionization and Lorentz force plates (roughly a 3 cm gap using the current fabricated geometry) may pose a problem for this EMFC concept. According to Jahn,[22] recombination rates depend on many properties including the species involved, temperature and density, etc. Ionized gas formed by high temperature dissociation demonstrates rapid recombination.[27] However, low temperature seeded ionization should see a lower recombination rate for two reasons. First, the lower temperature means that the intermolecular collisions between particles will be slower. Second, the heavy radicals of the ionized seed material will travel much slower relative to the free electrons after high voltage excitation. Very little literature appears to have been published about low temperature recombination of gases, especially in the presence of particle seeding. It is possible that nonequilibrium reactions formed between injected seed materials and air constituents during ionization may play a significant role in the recombination rate. Plasma spraying, as part of the thermal spraying industry, successfully seeds a plasma jet before it is accelerated past the anode and cathode region out to coat a surface. However, this spraying begins with a high temperature arc similar to a plasma torch. Cold plasma spraying, perhaps the most promising example to bolster our recombination presumptions, has been previously demonstrated.[28,29] If the recombination effects prove too difficult to overcome in the gap between the two plates, the power supplies can be merged into one plate with two separate pulsed power supplies.

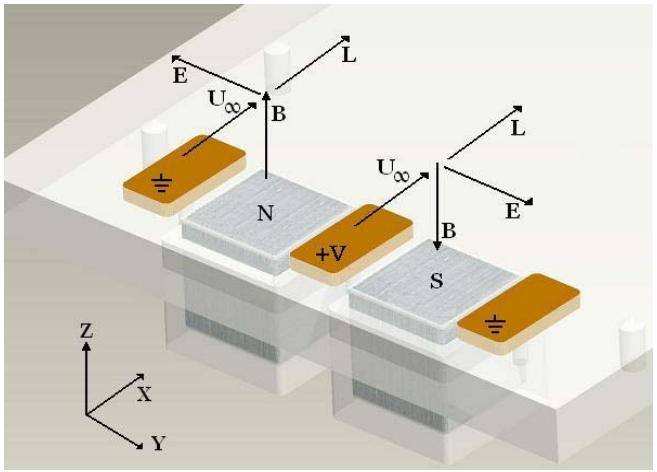

Figure 4. Schematic of a Lorentz force generator plate depicting the electromagnetic arrangement and force field interaction (flat plate material is translucent to show embedded magnets).

V. The Lorentz Force Plate

In order to create an accelerating or retarding Lorentz force, magnets and electrodes must be alternated across the width of the flat plate perpendicular to the flow direction. This arrangement results in each electrode pair crossing over one embedded magnet face, with the magnetic poles interchanged across the width. Grounded electrodes are placed at each end of the actuator to maintain a uniform force direction. Additionally, this may also prevent arcing from occurring to a tunnel wall or some other component. Figure 4 shows a schematic of the actuator design with a single electrode that delivers power, including an idealization of the electric and magnetic field directions. Here, the magnetic and electric fields are oriented in orthogonal directions above the actuator depending on the polarity of the magnet, with the fields crossing each other to produce the Lorentz body force in a single direction acting parallel with the flow. In Fig. 4, the magnets are

embedded a few mm below the plate material since exposing the magnets would produce arcing between them and the electrodes. Several generator plates have been fabricated, all with a width of about 4 inches to allow for testing in the UT Arlington low speed and supersonic wind tunnels.

Assuming a value of conductivity for the seeded flow makes the Lorentz force generator plate design fairly independent of the other components. Based on previous conductivity results after ionization of a pure gas[14] and one seeded with potassium carbonate,[17] the design of the actuator was based around $\sigma = 1$ mho/m. This value can change significantly depending on the success of the ionization actuator plate.

Previous work in EMFC have used electromagnets.[1,15] When compared with rare-earth magnets, electromagnets have considerable advantages for aerodynamics applications, namely, much stronger *B* field generation and applicability for high-temperature applications (i.e. scramjet inlets). However, permanent rare-earth magnets generate a higher *B* field with respect to their overall weight and do not require a dedicated power supply. Since the goal of this facility is to demonstrate the feasibility of the aforementioned three component configuration and reduce power consumption, rare-earth magnets were selected. Rare-earth, neodymium-iron-boron (NIB) magnets can reach surface field strengths of roughly 1.0 T, while those that fit into the size constraints of this Lorentz force generator range from 0.4 to 0.6 T.

A. Optimization Using Computational Magnetohydrodynamics

A computational magnetohydrodynamics program was used (see Acknowledgments) to provide a rough estimate of the actuator magnetic field strength, electric current and Lorentz body force for a two-dimensional array of magnets and electrodes assuming a perfect gas with a uniform conductivity profile. The inputs to the program are a free stream velocity, the flow conductivity, the electromagnetic geometry and the surface values of the electrode voltage and magnetic fields. The computational process begins with a laminar approximation of the boundary layer velocity profile over the flat plate, where *y* is the height above the plate:

$$U = U_\infty \left(1 - e^{\left(-\frac{4.6052 z}{\delta_{BL}} \right)} \right) \tag{3}$$

Assuming the magnetic field is curl and divergence free, it can be computed from a scalar potential:

$$\vec{B} = \nabla \psi \tag{4}$$

$$B_n = \frac{\partial \psi}{\partial n} \tag{5}$$

The electric field potential model uses the Poisson equation neglecting the Hall effect (although the Hall effect certainly can come into play in the experiments):

$$\vec{J} = \sigma \left(-\nabla \varphi + \vec{U} \times \vec{B} \right) \tag{6}$$

The MHD divergence-free current condition requires:

$$\nabla \cdot \vec{J} = 0 \tag{7}$$

$$\nabla \cdot \left(\sigma \nabla \varphi \right) = \nabla \cdot \left(\sigma \vec{U} \times \vec{B} \right) \tag{8}$$

Finally, the Lorentz force is calculated from:

$$\vec{L} = \sigma \left(\vec{E} + \vec{U} \times \vec{B} \right) \tag{9}$$

The magnet and electrode dimensions were optimized along the width of the plate to provide a maximum value of the Lorentz body force per unit power consumption of the generator. An estimate of the power supply was

extracted by averaging the two-dimensional value of J (A/m^2) over the width of the positive electrodes and scaling with an arbitrary streamwise length. The Lorentz force was averaged over an arbitrary height from the surface of the flat plate for the comparison. Generally, it appears that the width of the electrodes should be about half that of the magnets. This result will have to be experimentally validated.

As seen from the program and shown in Fig. 5, constructing a constant Lorentz force field across the width of a flat plate is very difficult due to the fact that the electric field is much higher near to the edges of the electrodes. The resulting Lorentz body force is also markedly higher near the ends of the electrodes and falls to zero in the gaps between the magnets and electrodes. However, the spikes in the Lorentz force occur over a very small volume with the rest of the force more uniform and increasing exponentially near to the surface of the flat plate.

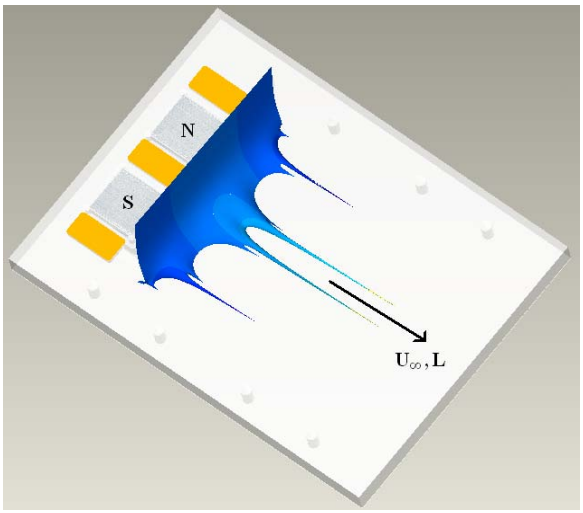

Figure 5. Overlay of the Lorentz force field geometry on the three electrode, two magnet generator.

B. Power Consumption

After the optimization strategy was used to select several electromagnetic geometry configurations, it was determined that a power supply capable of delivering tens of kW is needed for the Lorentz force plate. With a low electrode voltage desired to prohibit arcing, this results in a current draw from a few to 20 A. The most cost effective and simple way to generate this level of power is to use 12 VDC batteries connected in series. Car batteries have been used in similar EMFC experiments,[30] but smaller, high discharge motorcycle batteries were more suitable for this setup. Modular units of 10 batteries were assembled with interchangeable connector plates for use in series or charging in parallel. Fifteen of these 120 VDC modules have been assembled with the intention of using up to five for a single electrode. After limiting the current to 20 A with load resistors and circuit breakers, the power supply can accommodate three electrodes at 600 VDC for a total output of 36 kW. We estimate this power supply is therefore capable of producing an appreciable Lorentz force for conductivities ranging from 0.03-20 mho/m.

For safety, operation of the power supply is controlled using LabVIEW. To control the power supply, an analog

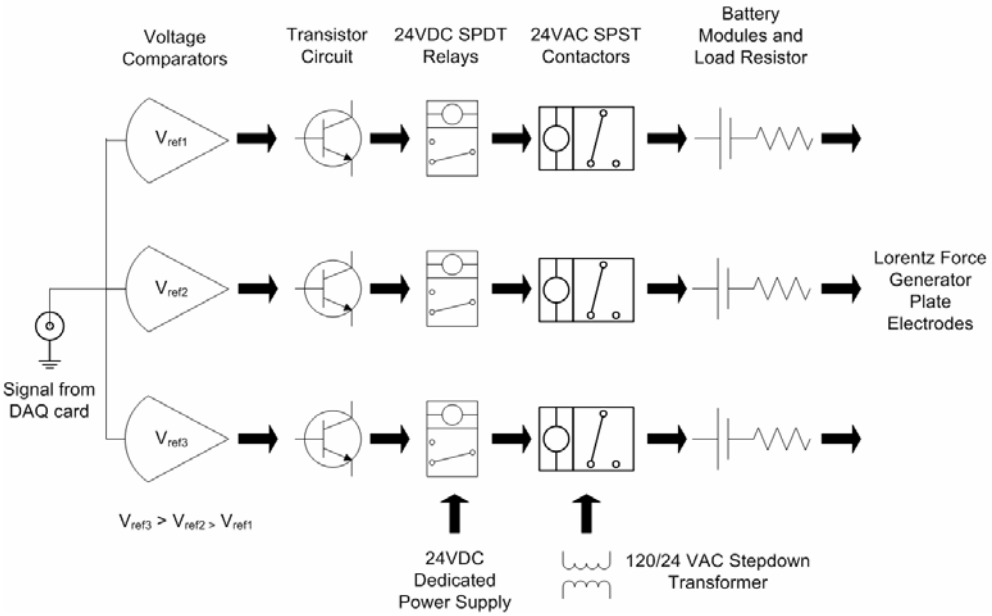

Figure 2. LabVIEW Lorentz force generator plate power supply control system schematic.

control voltage signal is first passed to a set of three voltage comparators. The three comparators correspond to a maximum of three active (+V) electrodes that can be used for the Lorentz force generator plate. The comparator reference voltages are set in numerical order so an increasing control voltage signal sent from LabVIEW will activate the electrodes one by one. Low power, computer compatible Darlington transistors are used to activate a 24 VDC SPDT relay, which in turn activates a 24 VAC SPST contactor in line with the main power supply for each electrode. The 24 VAC SPST contactors selected are typically used for air conditioning systems and can handle a large amount of power. They require a separate power supply, but that is easily satisfied with a 120 VAC power outlet and a transformer. Besides the battery modules, the rest of the electrode circuit consists of a load resistor to protect the batteries and a 20 A circuit breaker. LabVIEW also can act as a circuit breaker since it measures the power supply current and can deactivate the relays if it passes a user specified maximum value.

C. Power Supply Interaction

The power supply interaction between the Lorentz force and ionization plates is an important issue as far as experimental data collection is concerned. Since little is known about the recombination rate of the ionized particles, the current assumption is that the two plates should be placed as close as possible to each other for the particles to successfully be convected downstream and be influenced by the Lorentz force. However, for a separation under 2 cm, the +20 kV ionization electrodes will interact with the Lorentz force electrodes through spark or arc discharges. Although the power supply for ionization is limited to a current output of 15 mA, Fig. 7 shows the charge builds up over the electrodes in a capacitor-like manner and results in much higher current values during arcing. For arcing from the ionization plate electrodes to the Lorentz force electrodes, the resulting current measured across the Lorentz force generator power supply is far from negligible, resulting in an undesirable situation for accurate experimental measurements. This result is compounded by the fact that, for a continuous plasma cloud present over both plates, a conductive path between them will certainly exist and create an interaction current without arcing. Therefore, a case can be made for using a pulsed signal for ionization where the Lorentz force generator current measurement signals should only see brief periods of interaction from the +20 kV electrodes.

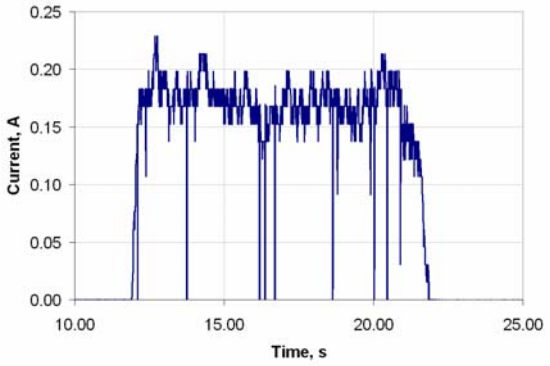

Figure 3. Typical current measurement taken during the interaction of the ionization and Lorentz force power supplies (the oscillations are spark discharges).

The interaction issue for this facility also shows that a pulsed RF signal, due to its alternating polarity, may be undesirable. Even during a short pulse at -20 kV, the conductive path between the power supplies will result in current directed back to the ionization power supply. Although that power supply is supported by a diode and fuse, the Lorentz force generator power output is too large to assume the ionization safety components will not be damaged.

VI. Preliminary Experimental Results

Benchtests have been conducted to estimate the feasibility of the ionization and Lorentz force plate concepts discussed thus far. Raised levels of conductivity are seen using seeding, but ionization by a DC electric field remains a difficult obstacle to overcome and a pulsed field may need to be used. The Lorentz force plate appears to work well, demonstrating an ability to control the motion of a salt water solution placed across the electrodes.

A. Seeding and the Ionization Actuator Plate

The ionization actuator plate was benchtested using a Glassman DC power supply with an output range of 0-20 kV and a maximum current draw of 15 mA. Voltage dependent current measurements were taken with the results shown in Fig. 8. Similar trends have been established.[16,23] The results indicate the presence of a non-visible discharge. As shown in Fig 8., even comparatively low voltages create a glow discharge as evidence through the current readings. Extrapolating on this result indicates a boundary layer flow velocity coupled with a higher fluid conductivity should increase the strength of the corona discharge.

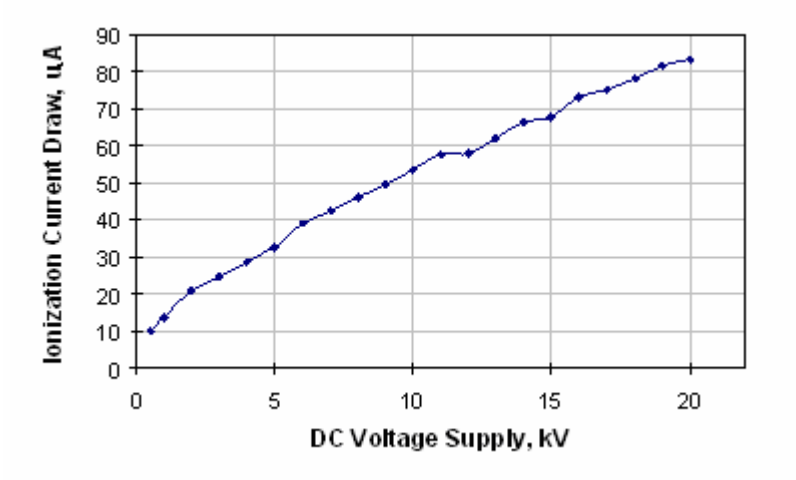

Figure 8. Ionization current vs DC supply voltage.

Beginning around 16 kV, corona discharge was visible to the unaided eye in a relatively dark room. At 20 kV, a uniform corona was intermittently visible across the electrodes. The faint glow discharge between electrodes was difficult to photograph, however a distinct outline of the corona can be seen in Fig. 9. Next, a flow was established using a jet of pressurized air directed parallel to the surface of the plate. While the pressurized jet appeared to convect the visible corona discharge away, no measurements can yet be taken to determine if free ions are present downstream. Future studies will focus on the ionization and recombination effects downstream of the ionization plate.

Next, a 3M (14.92 Wt.% NaCl) solution of salt/water was introduced across the ionization plate with the pressurized jet. As calculated in the next section, the average conductivity of the solution was estimated to be 0.25 mho/m. Unfortunately, these experiments were plagued with arcing due to the introduction of an ionic solution into a corona discharge. This shows that attempting high voltage DC boundary layer ionization with a low-speed, ionic solution can be problematic. Research using DC voltage for supersonic ionization by flow discharge shows more promise.[31] The conductivity of a corona discharge at low and high speeds for pure gases is simply orders magnitude below the desired seeded flow values for this facility, making stable DC field ionization by our facility very difficult. There exists a need for a pulsed glow or spark discharge using high frequency square waves at this point in the development.

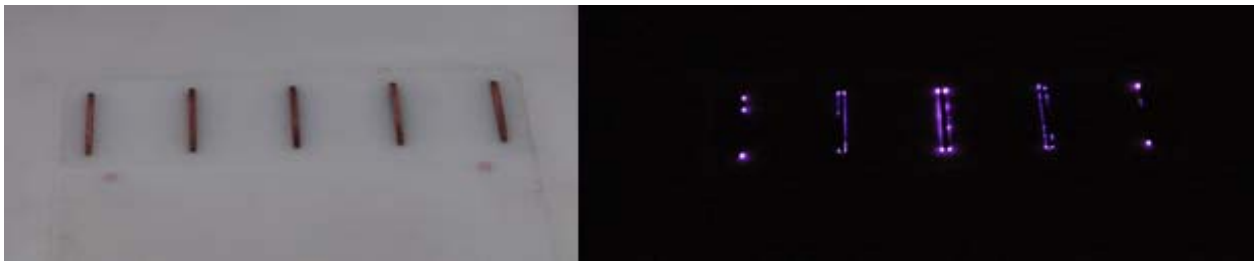

Figure 9. Ionization plate setup and corona discharge at 20 kV.

B. Actuation of the Lorentz Force Plate

The Lorentz force plate was bench tested using a 3 M salt/water spread across its surface. Blue dye was added for additional visualization of the mixture as shown in Fig. 10. The power supply was limited in this case to 120 VDC coupled with an 11.6 Ω load resistor. The result upon activation of the power supply was an instantaneous movement forward by most of the liquid layer.

If there was air flowing from right to left in the figure, the result of this electromagnetic configuration would be a retarding force. Note that the upstream ionization electrodes are shown in the figure and were removed from their ground so as to not interfere with the propagation of the mixture. The voltage was applied only to the center electrode with the two others serving as ground to direct the current flow needed for the Lorentz force to act in one direction. The width between the ground electrodes in the figure is about 4 inches. Figures 11 and 12 show the voltage, current and power measurements across the electrodes charted as a function of time. The power supply was only activated for a small amount of time since the mixture boils quickly due to joule heating. Figure 11 shows that the current spikes to 1.5 A before falling to a more steady value of roughly 0.7 A., effectively because most of the conductive layer moves off the plate the moment the power supply is turned on. The geometry of the layer as it moves forward was expected to follow the Lorentz force field geometry of the computational results (see Fig. 5), but

it appears that viscous effects of the water and hydrophobic nature of the plate material caused the layer to build up more towards the middle of the electrode gaps.

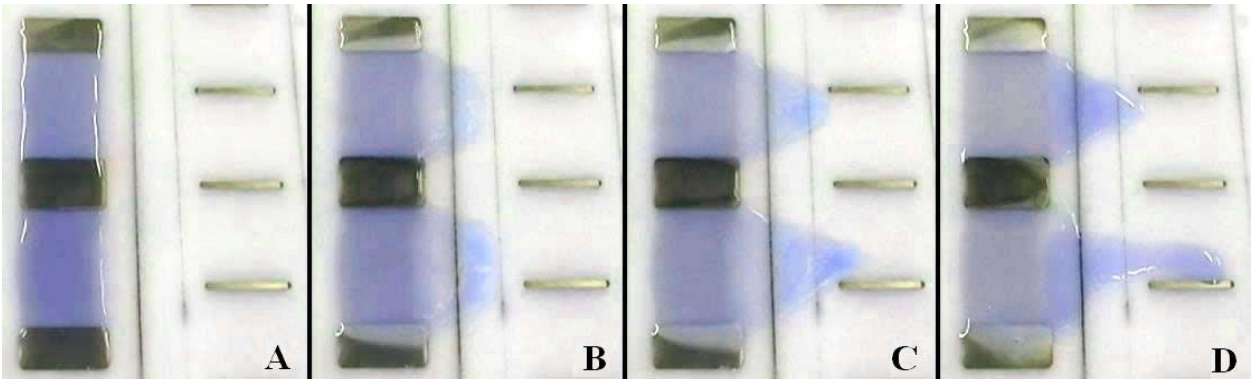

Figure 10. Frame by frame pictures of the Lorentz force generator plate actuation using a salt water mixture and dye for visualization.

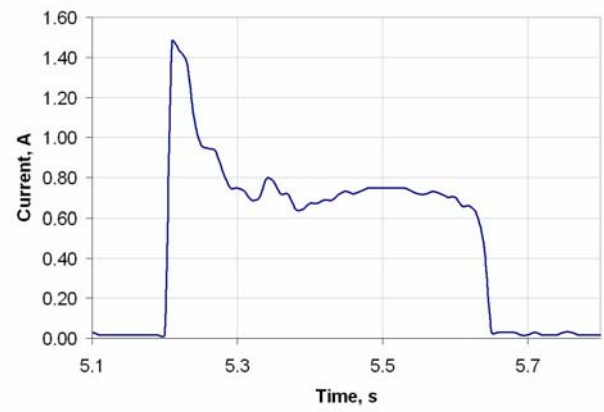

Figure 11. Current versus time during the actuation of the Lorentz force generator plate.

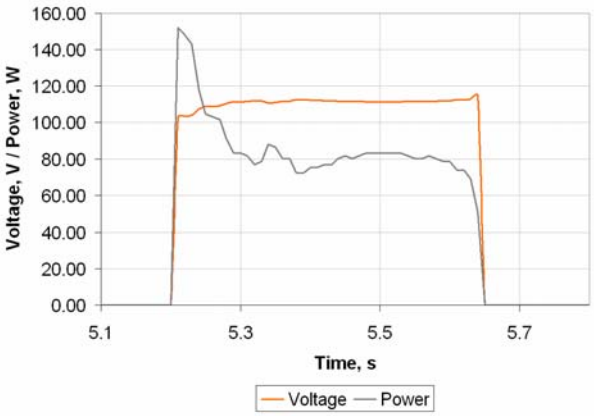

Figure 12. Voltage and Power versus time during the Lorentz force actuation.

Using the geometry and the information from the figures above, it is possible to approximate the average conductivity, Lorentz force and acceleration for the mixture when the power supply was activated. Using $V = IR$, the resistance across each gap between the electrodes is 140 Ω. The conductance is the inverse of the resistance value, and dividing it by the length of the electrode gap yields $\sigma = 0.25$ mho/m. The value is far less than the conductivity of sea water, indicating that only a small amount of sea salt was used in our mixture. Higher sea salt concentrations were used next in identical experiments which yielded current spikes up to 6 A. Since σ scales linearly with the current draw of the Lorentz force generator, the 6 A value indicates that σ reached about 1 mho/m for that case. Although the Lorentz force is very nonlinear as shown by the computational result, an order of magnitude approximation begins by defining a control volume over the electrode gap with a height equal to the height of the conducting layer placed on the plate. An F. W. Bell 5180 Hall effect gauss meter was used to measure the three-dimensional magnetic field present over the configuration of Fig. 9. Averaging the magnetic field over a control volume height of 3 mm yields $B \approx 0.3$ T. The electric field strength can be roughly averaged using the computational code results for E in the middle of the electrode gap, producing $E \approx 2000$ V/m. Since there is no flow velocity in this case, $L \approx \sigma E = 500$ N/m^3. Note that this Lorentz force approximation is independent of B, but the magnetic field is still integral to the magnitude of the Lorentz force. Multiplying the body force by the control volume yields $L \approx 4$ mN. Neglecting surface tension and friction forces and solving for $a = F/m$ results in an instantaneous acceleration of about 0.5 m/s when the power supply is activated. Obviously, this value rises tremendously using air instead of water because of the differences in density.

One interesting phenomena observed during the testing of the Lorentz force generator plate is the presence of vortex dipoles within the conductive salt water. Upon removing the salt from the solution and activating the electrodes with only distilled water and a small amount of dye, the vortex dipoles were visualized. Apparently, the dye used contains a very small amount of conductivity, but not enough to generate a Lorentz force capable of displacing the fluid off of the electrodes. No appreciable current from the power supply was detected. The dye rotated inside the water and resulted in the image shown in Fig. 13. Although these dipoles have a strong effect in the salt water solution, they are expected to have a negligible impact on the conductive seed-air experiments since they only influence viscous solutions.[32]

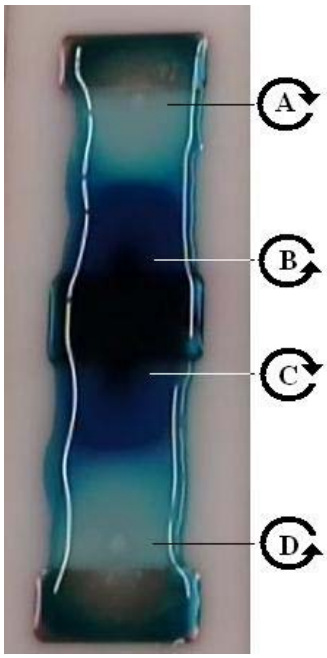

Figure 13. Visualization of two vortex dipoles.

VII. Future Work and Conclusions

The boundary layer flow conductivity and resulting electromagnetic Lorentz force field magnitude distribution across the flat plate are two difficult EMFC parameters to accurately measure. Extrapolation of the conductivity from MHD relations and power supply measurements appears to be a viable method as seen in the salt water experiments, with more precise calculation techniques available.[33] The Lorentz force field can be extrapolated in two different ways. First, more benchtests using the saltwater solution can be used to validate the accuracy of the computational program predictions, upon which the Lorentz force field magnitude distribution will be better trusted. Second, three dimensional magnetic and electric fields can be mapped over the surface of the Lorentz force generator plates using the F. W. Bell 5180 gauss meter and a current field probe. With these fields and the conductivity, a Lorentz force vector field can be calculated. The sought after aerodynamic data, the change in pressure over the surface of the plate, will be measured using pressure transducers flush mounted to the surface of the Lorentz force generator plate. PIV measurements will be used to gain a better understanding the EMFC flow dynamics.

In conclusion, it has become quite obvious during the development of this facility that a successful design requires a multi-disciplinary approach between the fields of aerodynamics, magnetohydrodynamics and the physics and chemistry of weakly ionized gases. The benchtesting of this facility has shown two technical issues to overcome, namely, the vaguely understood nature of conductive particle recombination between the ionization and Lorentz force plates and the optimization of a high voltage signal that can both generate the sought after seed-air conductivity range and withstand the proclivity for uncontrollable arcing at those voltage and conductivity levels. A methodology has been developed to work with these issues. A variety of feasible seeding mechanisms and ionization strategies have been seen throughout the development process of this facility and reported throughout the literature, indicating promise for increasing boundary layer conductivity through particle seeding.

Acknowledgments

We would like to thank Dr. Ramakanth Munipalli of HyPerComp, Inc., for providing the computer program for estimating the magnetic field strength, electric current, and Lorentz force distribution for a 2D array of magnets and electrodes. We would also like to thank Philip Panicker for many useful discussions involving the design and use of high power electronics. This work was partly supported by the Texas Advanced Research Program, Project No. 003656-0013-2006.

References

[1]Shang, J.S., "Recent Research in Magneto-aerodynamics," *Progress in Aerospace Sciences*, Vol. 37, No. 1, 2001, pp. 1–20.

[2]Meyer, R., Chintala, N., Bystricky, B., Hicks, A., Cundy, M., Lempert, W.R. and Adamovich, I.V., "Lorentz Force Effects on a Supersonic Ionized Boundary Layer," AIAA Paper 2004-0510, 2004.

[3]Gaitonde, D.V. and Tumin, A., "Electromagnetic Control of Unstable Disturbances in a Weakly Ionized Entropy Layer," AIAA Paper 2004-0511, 2004.

[4]Kimmel, R.L. and Hayes, J.R., "Effect of Magnetic Fields on Surface Plasma Discharges at Mach 5," *Journal of Spacecraft and Rockets*, Vol. 43, No. 6, 2006, pp. 1340-1346.

[5]Shin, J., Narayanaswamy, V., Laxminarayan, R.L. and Clemens, N.T., "Characterization of a Direct-Current Glow Plasma Actuator in Low-Pressure Supersonic Flow," *AIAA Journal*, Vol. 45, No. 7, 2007, pp. 1597-1605.

[6]Corke, T.C., and Post M.L., "Overview of Plasma Flow Control: Concepts, Optimization, and Applications," AIAA Paper 2005-0563, 2005.
[7]Menart, J., Henderson, S., Atzbach, C., Shang, J., Kimmel, R., and Hayes, J., "Study of Surface and Volumetric Heating Effects in a Mach 5 Flow," AIAA Paper 2004-2662, 2004.
[8]Bityurin, V.A., Bocharov, A.N., and Lineberry, J., "MHD Flow Control in Hypersonic Flight," AIAA Paper 2005-3225, 2005.
[9]Ring, L., "RDHWT/MARIAH II Systems Integration Studies Review," AIAA Paper 2004-2486, 2004.
[10]Menart, J., Shang, J., Atzbach, C., Magoteaux, S., Slagel, M., and Bilheimer, B., "Total Drag and Lift Measurements in a Mach 5 Flow Affected by a Plasma Discharge and a Magnetic Field," AIAA Paper 2005-0947, 2005.
[11]Weier, T., and Gerbeth, G., "Control of Separated Flows by Time Periodic Lorentz Forces," *European Journal of Mechanics B/Fluids*, Vol. 23, No. 6, 2001, pp. 835–849.
[12]Dietiker, J-F, and Hoffmann K.A., "Numerical Simulation of Magnetohydrodynamic Flows," *Journal of Spacecraft and Rockets*, Vol. 41, No. 4, 2004, pp. 592–602.
[13]Macheret, S.O., Shneider, M.N., and Miles, R.B., "Magnetohydrodynamic and Electrohydrodynamic Control of Hypersonic Flows of Weakly Ionized Plasmas," *AIAA Journal*, Vol. 42, No. 7, 2004, pp. 1378-1387.
[14]Kimmel, R.L., Hayes, J.R., Menart, J.A., and Shang, J.S., "Effect of Magnetic Fields on Surface Plasma Discharges at Mach 5," AIAA Paper 2004-2661, 2004.
[15]Nishihara, M., Jiang, N., Rich, J.W., Lempert, W.R., and Adamovich, I.V., "Low-temperature Supersonic Boundary Layer Control using Repetitively Pulsed MHD Forcing," AIAA Paper 2005-5178, 2005.
[16]Panicker, P.K., Satyanand, U.S., Lu, F.K., Emanuel, G., and Svihel, B.T., "Development of Corona Discharge Apparatus for Supersonic Flow," AIAA Paper 2003-6925, 2003.
[17]Lu, F.K., Hsuan-Cheng, L. and Wilson, D.R., "Electrical Conductivity Channel for a Shock Tube," *Measurement Science and Technology*, Vol. 16, No. 9, 2005, pp. 1730-1740.
[18]Narasimha, R. and Prasad, S.N., "Leading Edge Shape for Flat Plate Boundary Layer Studies," *Experiments in Fluids*, Vol. 17, No. 5, 1994, pp.358-360.
[19]Compton, D.A. and Eaton, J.K., "Near-Wall Measurements in a Three-Dimensional Turbulent Boundary Layer," *Journal of Fluid Mechanics*, Vol. 350, 1997, pp. 189-208.
[20]Kruse, M. and Wagner, S., "Visualization and Laser Doppler Measurements of the Development of Lambda Vortices in Laminar-Turbulent Transition," *Measurement Science and Technology*, Vol. 9, No. 5, 1998, pp. 659-669.
[21]Barrett, R.V., "Transition detection for laminar flow aircraft using microphones beneath the surface of laser drilled suction panels," *Journal of Aerospace Engineering*, Vol. 214, No. 3, 2000, pp. 143.
[22]Jahn, R.B., *Physics of Electric Propulsion*, Dover, 1996, p. 339.
[23]von Engel, A., *Ionized Gases*, Oxford University Press, London, 1955.
[24]Roth, J. R. and Dai, X., "Optimization of the Aerodynamic Plasma Actuator as an Electrohydrodynamic (EHD) Electrical Device," AIAA Paper 2006-1203, 2006.
[25]Utkin, Y. G., Keshav, S., Kim, J.-H., Kastner, J., Adamovich, I. V. and Samimy, M., "Development and use of localized arc filament plasma actuators for high-speed flow control," *J. Phys. D: Appl. Phys.*, Vol. 40, 2005, pp. 685-694.
[26]Bäcker, H. and Bradley, J. W., "Observations of the Long-term Plasma Evolution in a Pulsed DC Magnetron Discharge," *Plasma Sources Sci. Technol*, Vol 14, 2005, pp. 419-431.
[27]Vincenti, W. G. and Kruger C. H., *Introduction to Physical Gas Dynamics*, Kreiger, New York, 1965.
[28]Koinuma, H., Ohkubo, H., Hashimoto, T., Inomata, K., Shiraishi, T., Miyanaga, A. and Hayashi, S., "Development and Application of a Microbeam Plasma Generator," *Appl. Phys. Lett.,* Vol. 60, No. 7, 1992, pp. 816-817.
[29]Schütze, A., Jeong, J. Y., Babayan, S. E., Park, J., Selwyn, G. S., and Hicks, R. F., "The Atmospheric-Pressure Plasma Jet: A Review and Comparison to Other Plasma Sources," *IEEE Transactions on Plasma Science*, Vol. 26, No. 6, 1998, pp. 1685-1694.
[30]Rittenhouse, L. E., Pigott, J. C., Whoric, J. M. and Wilson, D. R., ARO, Inc., "Theoretical and Experimental Results with a Linear Magnetohydrodynamic Accelerator Operated in the Hall Current Neutralized Mode," AEDC-TR-67-150, 1967.
[31]Menart, J., Shang, J., Kimmel, R. and Hayes, J., "Effects of Magnetic Fields on Plasmas Generated in a Mach 5 Wind Tunnel," AIAA Paper 2003-4165, 2003.
[32]Afanasyev, Y. D. and Korabel, V. N., "Starting Vortex Dipoles in a Viscous Fluid: Asymptotic Theory, Numerical Simulations, and Laboratory Experiments," *Physics of Fluids*, Vol. 16, No. 11, 2004, pp. 3850-3858.
[33]Meyer, R., Nishihara, M., Hicks, A., Chintala, N., Cundy, M., Lempert, W. R., Adamovich, I. V., and Gogineni, S., "Measurements of Flow Conductivity and Density Fluctuations in Supersonic Nonequilibrium Magnetohydrodynamic Flows," *AIAA Journal*, Vol. 43, No. 9, 2005, pp. 1923-1930.